

E Letts

MODELLING FUSED SINGLE MODE FIBRE COUPLERS.

F.P. Payne. C.D. Hussey. M.S. Yataki.

Department of Electronics and Information Engineering
The University
Southampton
SO9 5NH
Hampshire.

INDEXING TERMS: Single Mode Fibres, Single mode fibre couplers.

ABSTRACT

The fused single mode tapered coupler is successfully modelled by assuming that the neck section of the coupler can be represented by a rectangular dielectric waveguide. Guidance is provided at the glass to air (or external medium) boundary and the cores are neglected. The mechanism of field detachment from the cores is outlined and the coupler characteristics are derived from the interference between the two lowest order modes of the large waveguide.

INTRODUCTION

The fused tapered coupler is perhaps the most successful of the single mode couplers for achieving stable low-loss operation. ^{1,2,3.}

The theory of evanescent field coupling, which can adequately describe the behaviour of the etched or polished coupler ^{4,5}, has been found to be inappropriate when applied to the fused tapered coupler. ^{2,6.}

The problem with the single mode tapered coupler is that at some point along the taper, the propagating field becomes detached⁷ from the core of the fibre so that in the neck section of the taper the field is guided by the boundary between the cladding and the external medium (i.e. air or some suitable potting material), ^{2,6,8} while the cores are reduced to such an extent that they can be neglected. ⁶

Coupling takes place through the interaction of the modes of the composite waveguide formed at the neck section of the coupler by the fusion of the two fibres. While this idea has been tentatively suggested and explored by some authors ^{2,6} no simple or intuitive model of the process has emerged. Such a model is essential if we are to optimise coupler fabrication and perhaps more importantly if we are to exploit fully the modulating and switching capabilities of the fused tapered coupler. ^{2,8}

In this letter we propose the simplest possible model for the single-mode fused tapered coupler. Field detachment in the taper is analysed remarkably accurately using ray optics (in close analogy with multimode tapers). The neck section of the taper is modelled by a rectangular multimode waveguide with only the lowest order symmetric and antisymmetric modes excited by the incoming field.

More detailed analysis and comparison with experimental results are presented elsewhere. ¹¹

THE MODEL.

The fused tapered couplers as made at Southampton have a structure similar to that of Fig 1(a). The outer taper angle α lies in the range 0.1 - 0.3°. The neck section CD between the two tapers is approximately parallel with a length up to 2 cms. An LP₀₁ mode on an input arm of the coupler is initially guided by the fibre core. On entering the taper section it sees a core of gradually reducing radius. At any point on the fibre the mode can be decomposed locally into plane waves. This local plane wave decomposition can accurately describe the propagation of the LP₀₁ mode, even for low V values. The mode will be guided by the core until its local angle of incidence at the core-cladding boundary equals the critical angle. This occurs when:

$$\frac{\beta^2 - n_2^2 k^2}{(n_1^2 - n_2^2) k^2} = \frac{2 \alpha_c n_2}{(n_1^2 - n_2^2)^{1/2}} \quad (1)$$

where α_c is the core taper angle.

At this point the LP₀₁ mode will refract out of the core and must be considered a field of the entire cross section of the coupler.⁶

It is found from eq (1) that for the single mode tapers contained in our couplers, (NA= 0.09,) field detachment occurs close to the neck of the taper.

We postulate that the main coupling action is due to interference between the two lowest order modes of the section CD between the tapers, the entire cross section of which is now considered as a waveguide of refractive index n_2 in a medium n_3 . This has a dumb bell cross section, shown dotted in Fig 1(b). The smallest cross section of our couplers has $a = 2.5 \mu\text{m}$. Assuming that n_2 is that of silica (1.458) and the potting medium n_3 is 1.42 we find that V for this waveguide is of order 8 at $\lambda = 633\text{nm}$. At such large values of V the propagation constants and fields of the two lowest order modes are insensitive to the detailed shape of the cross section, and we propose to model it with a rectangular dielectric waveguide, as shown in Fig 1(b). The error involved should be very small.

ANALYSIS:

We consider interference between the lowest order even and odd modes of the rectangular guide. It is straightforward to derive accurate analytic expressions for the propagation constants of these modes.¹⁰

If the power of one of the output ports is described by

$$P = P_0 \sin^2 (cL)$$

then it can be shown that

$$c = \frac{3\pi\lambda}{32n_2a^2} \cdot \frac{1}{(1+1/V)^2} \quad (2)$$

where $V \equiv a k (\eta_2^2 - \eta_3^2)^{1/2}$

RESULTS:

Equation (2) is a particularly simple description of the coupler. The wavelength dependence of the output power is predicted to vary periodically with λ . For a previously measured coupler², $a = 2.63\mu\text{m}$, $L = 15\text{ mm}$, $n_2 = 1.458$ and $n_3 = 1.42$. The predicted output is shown in Fig. 2. Since V also depends on λ the period $\Delta\lambda$ is not quite constant and can be shown to be given by

$$\Delta\lambda = \frac{32n_2a^2}{3L} \cdot \frac{(1+1/V)^3}{(1-1/V)} \quad (3)$$

at two different wavelengths the predicted and measured $\Delta\lambda$ corresponding to Fig. 2 are

| λ (nm) | $\Delta\lambda$ (eq.3) nm | $\Delta\lambda$ (measured) nm |
|----------------|---------------------------|-------------------------------|
| 500 | 10.2 | 11.3 |
| 700 | 11.8 | 13.2 |

The agreement is very good and even the observed small increase in $\Delta\lambda$ is accounted for. Similar agreement is obtained for other couplers. This adds support to our assumption of coupling between the two lowest order modes only.

The effects on the output power of changing the external n_3 are described by the V dependence of eq.(2). In particular eq. (2) predicts a strong variation when L/a^2 is large and n_3 is close to n_2 . This is again consistent with experiment and in Fig.3 we show the variation of output power with n_3 for two different couplers with $L = 10\text{mm}$ and taper ratios of 10 and 20. The initial fibre diameter was $105\mu\text{m}$. The predicted behaviour is very similar to that measured².

DISCUSSION:

In deriving eq (2) we have assumed only two modes in the coupling region. The observed periodic variation of output power with λ supports this assumption. If more than two modes were present we would expect to see several periods in the λ dependence and this is not observed. The small increase in period with increasing λ that is measured is also correctly predicted by this model.

In a more refined analysis we can allow for coupling in the tapers¹¹. This involves integrating eq. (2) with respect to a along the taper. Since the analytic form of (2) is particularly simple this presents no difficulties. A further refinement will be to include polarisation effects in the coupler.¹¹ The two orthogonal polarisations have slightly different beat lengths and in very long couplers this results in a modulation of the wavelength dependence.¹²

In conclusion, we have presented a simple model for the taper coupler. It explicitly displays the dependence on physical parameters and should prove useful in the practical design of couplers, and coupler based devices.

ACKNOWLEDGEMENTS:

We would like to thank Dr.D.N. Payne, R.J. Mears and F. Martinez for useful discussions. This research was supported by the S.E.R.C.

REFERENCES:

1. KAWASAKI, B.S., HILL, K.D., LAMONT, R.G.: "Biconical taper single-mode fibre coupler" *App. Optics*, 1981, 6, pp 327 - 328.
2. de FERNEL, F., RAGDALE, C.M., MEARS, R.J.: "Analysis of single mode fused tapered couplers". *I.E.E. Part J.* 1984, 131, pp 221 - 228.
3. BRICHENO, T., FIELDING, A.: "Stable Low-loss single mode couplers". *Electron. Lett.*, 1984, 20 pp 230 - 232.
4. TRAN, DAWH. C., KOO, P. KEE., SHEEM. SAN G.K.,: "Single mode fiber directional couplers fabricated by twist etching techniques (Stabilization)". *I.E.E.E., Vol. QE - 17* (1981) pp 988 - 990.
5. DIGONNET, M., SHAW. H.S.: "Wavelength Multiplexing in single mode fiber couplers" *App. Opt.* (1983) Vol. 22, pp 484 - 491.
6. BURES, J., LACROIX, S., LAPIERRE. J., "Analyse d'un coupleur bidirectionnel à fibres optiques monomodes fusionnées". *App. Opt.* (1983) Vol. 22. pp 1918 - 1922.
7. BEAUMONT, A.R., "Tapers in single-mode optical fibres", University of Southampton Final Year Project Report, May 1984.
8. BURES. J., LACROIX, S., VEILLEUX, C., LAPIERRE. J., "Some particular properties of monomodefused fiber couplers". *App. Opt.* (1984) Vol 23, pp 968 - 969.
9. HARTOG, A.H. and ADAMS, M.J., "On the accuracy of the W K B approximation in optical dielectric waveguides". *Optical and Quantum Electronics* (1977), Vol.9, pp 223 - 232.
10. MARCATILI, E.A.J. "Dielectric rectangular waveguide and directional coupler for integrated optics". *Bell Syst. Tech. J.*, (1969) Vol 48, pp 2071 - 2102.

11. PAYNE, F.P., HUSSEY, C.D., YATAKI, M.S., "Experimental and theoretical analysis of fused single mode fibre couplers", to be published.
12. YATAKI, M.S., VARNHAM, M.P., PAYNE, D.N., "Fabrication and properties of very long fused taper couplers", Proc. 8th Optical Fibre Conference, San Diego, 1985.

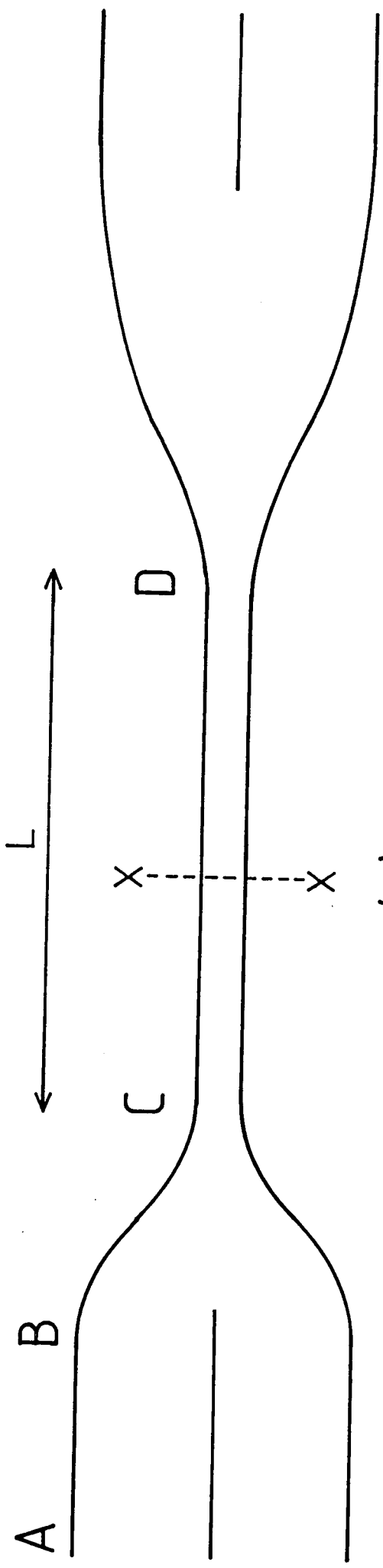
FIGURE CAPTIONS.

1. (a) Approximate shape of a fused taper coupler.

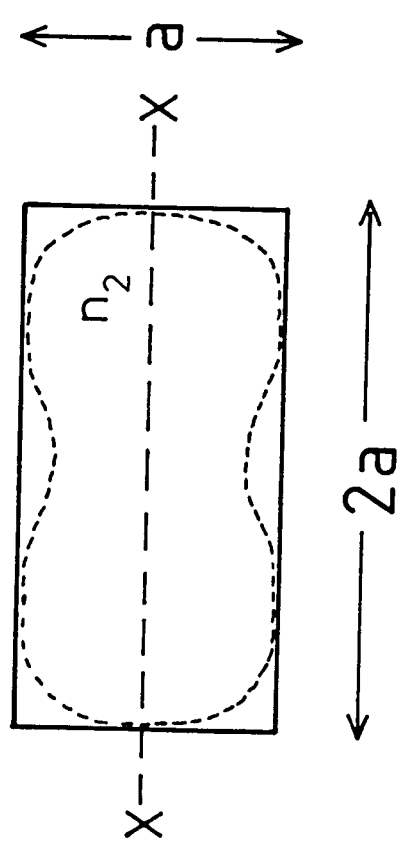
(b) A cross section of the coupler through XX has the shape shown dotted. The rectangle is the approximation used to model this at high $V = ak(n_2^2 - n_3^2)^{1/2}$.

2. Prediction of the variation of output power with wavelength for a coupler with $a = 2.63\mu\text{m}$, $L = 15\text{mm}$, $n_2 = 1.458$ and $n_3 = 1.42$. This corresponds to the experimental curve Fig 8(c) of ref. 2.

3. Variation of output power with external refractive index n_3 for two couplers with different taper ratios T_R . This corresponds to the experimental curve Fig 10 of ref. 2.



(a)



(b)

Fig.1

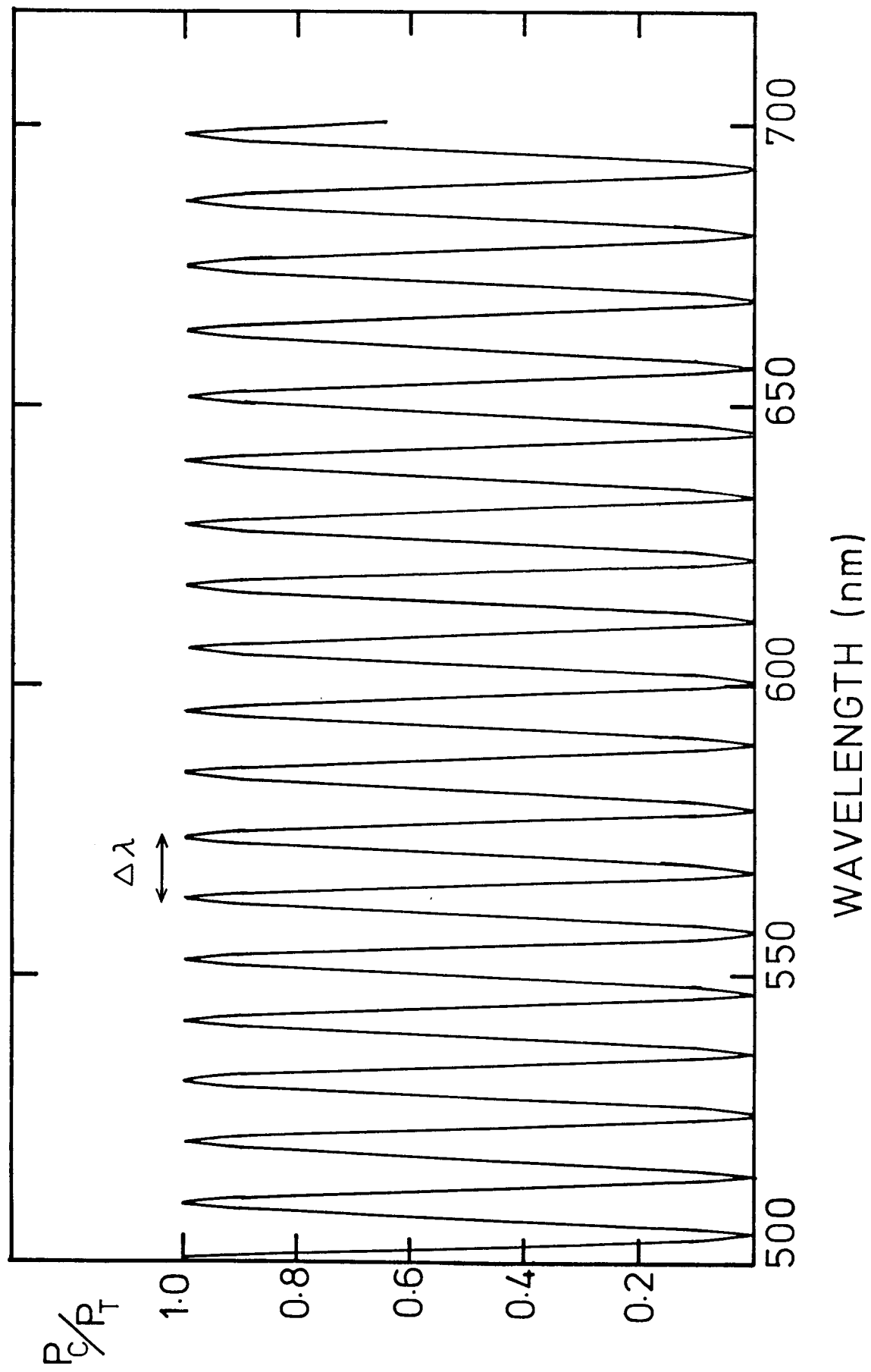
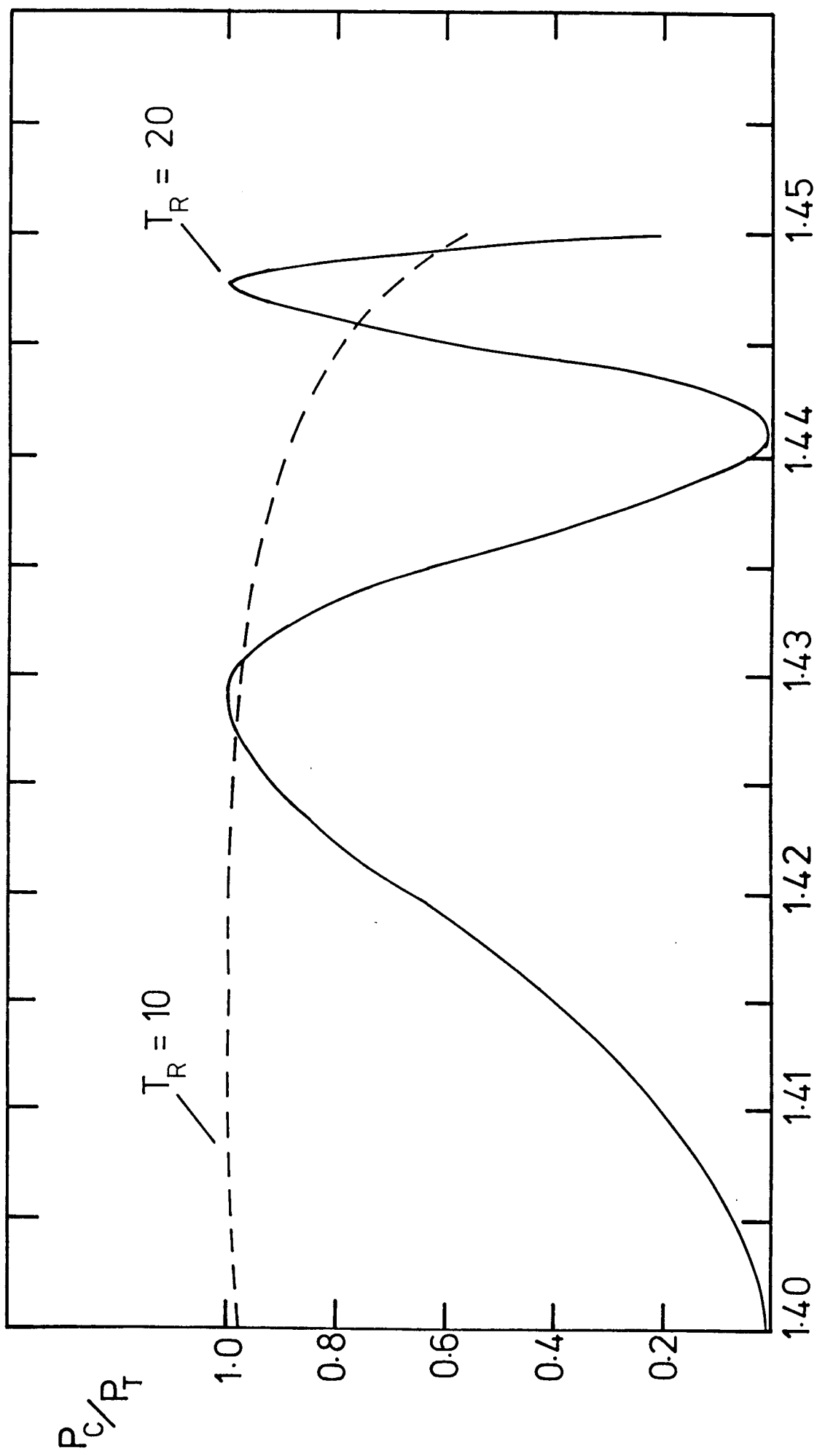


Fig.2



EXTERNAL REFRACTIVE INDEX n_3

Fig.3